

**TESTING MEM WITH DIQUARK AND THERMAL MESON  
CORRELATION FUNCTIONS<sup>a, b</sup>**

I. Wetzorke and F. Karsch  
*Fakultät für Physik*  
*Universität Bielefeld*  
*33615 Bielefeld, Germany*

When applying the maximum entropy method (MEM) to the analysis of hadron correlation functions in QCD a central issue is to understand to what extent this method can distinguish bound states, resonances and continuum contributions to spectral functions. We discuss these issues by analyzing meson and diquark correlation functions at zero temperature as well as free quark anti-quark correlators. The latter test the applicability of MEM to high temperature QCD.

**1 Principles of MEM**

The **MAXIMUM ENTROPY METHOD** is a common technique in condensed matter physics, image reconstruction and astronomy<sup>1</sup>. In lattice QCD it has been applied recently to analyze meson correlation functions at zero temperature<sup>2</sup>. It could be demonstrated that this method correctly detects the location of poles in the correlation function and, moreover, is sensitive to the contribution of higher excited states to the correlators.

Starting from correlation functions,  $D(\tau)$ , in Euclidean time which are calculated on the lattice at a discrete set of time separations,  $\{\tau_k\}_{k=1}^{N_\tau}$ , the application of MEM allows to extract the *most probable* spectral function without any assumptions about the spectral shape. This is an important key to access real time correlation functions and other dynamical quantities through lattice calculations. Of course, the essential bottleneck is that one has to specify what is meant by the *most probable spectral function*: MEM is based on **Bayes theorem of conditional probability**, which yields the most probable result for the spectral function  $A(\omega)$  given the dataset  $D(\tau)$  and all prior knowledge  $H$  (e.g. positivity of  $A(\omega)$ )<sup>1,3</sup>:

$$P[A|DH] \sim P[D|AH]P[A|H] \quad \text{with} \quad \begin{aligned} P[D|AH] &\sim \exp(-L) \\ P[A|H] &\sim \exp(\alpha S) \end{aligned} \quad (1)$$

<sup>a</sup>Work supported by the TMR-Network grant ERBFMRX-CT-970122 and the DFG grant Ka 1198/4-1.

<sup>b</sup>Presented at the Conference on Strong and Electroweak Matter (SEWM 2000), Marseille, France, 14-17 June 2000.

The **Likelihood function**,  $L$ , is chosen as the usual  $\chi^2$  distribution

$$L = \frac{1}{2}\chi^2 = \frac{1}{2} \sum (F(\tau_i) - D(\tau_i)) C_{ij}^{-1} (F(\tau_j) - D(\tau_j))$$

with  $C_{ij}$  denoting the symmetric covariance matrix constructed from the data sample and  $F(\tau) = \int d\omega K(\tau, \omega) A(\omega)$  is the *fit function* in terms of a predefined kernel  $K(\tau, \omega)$  and the spectral function  $A(\omega) \equiv \rho(\omega) \omega^2$ . For an unnormalized probability function  $A(\omega)$  we can parametrize the **entropy**,

$$S = \int d\omega [A(\omega) - m(\omega) - A(\omega) \log(\frac{A(\omega)}{m(\omega)})] ,$$

where  $m(\omega) = m_0 \omega^2$  is the *default model*, i.e. the initial ansatz for  $A(\omega)$ . The default model incorporates our knowledge about the short distance behaviour of meson correlation functions<sup>2</sup>, which in leading order perturbation theory are proportional to  $\omega^2$ . The real and positive factor  $\alpha$  controls the relative weight between the entropy (default model) and Likelihood function (data) appearing in Eq. 1.

The most probable spectral function  $\hat{A}_\alpha(\omega)$  is then obtained by maximizing  $Q \equiv \alpha S - L$  for given  $\alpha$  and the final spectral function  $\bar{A}(\omega)$  is determined from a weighted average over  $\alpha$ :

$$\bar{A}(\omega) = \int \mathcal{D}A d\alpha A(\omega) P[A|DH] P[\alpha|D] \simeq \int d\alpha \hat{A}_\alpha(\omega) P[\alpha|D] .$$

Usually it turns out that the weight factor  $P[\alpha|D]$  is sharply peaked around a unique value  $\hat{\alpha}$ .

In the following we will apply this general framework to analyze zero-momentum meson and diquark correlation functions in Euclidean time,  $D(\tau)$ . The correlators are calculated in quenched QCD on lattices with temporal extent  $N_\tau$ . They can be expressed in terms of the spectral function  $A(\omega)$ ,

$$D(\tau) = \int d^3x \langle \mathcal{O}^\dagger(\tau, \vec{x}) \mathcal{O}(0, \vec{0}) \rangle = \int d\omega K(\tau, \omega) A(\omega) .$$

Here the kernel  $K(\tau, \omega)$  is taken to be proportional to the Fourier transform of a free boson propagator,

$$K(\tau, \omega) = e^{-\tau\omega} / (1 - e^{-N_\tau\omega}) .$$

The computational intensive part of MEM is the maximization of  $Q = \alpha S - L$  in the functional space of  $A(\omega)$ , for which one typically uses a few hundred degrees of freedom. A **Singular Value Decomposition** (SVD) of the kernel  $K(\tau, \omega)$  was performed to reduce the parameter space.

## 2 Details of the Simulation

For our tests of MEM we used data from a previous spectrum calculation<sup>4</sup> in quenched QCD with Wilson fermions on lattices of the size  $16^3 \times 30$  and  $16^3 \times 32$ . In order to study also diquark correlation functions Landau gauge fixing has been performed on the larger lattice. In the gluon sector we use the Symanzik improved (1,2) action, which eliminates  $\mathcal{O}(a^2)$  cut-off effects. In the fermion sector we use the  $\mathcal{O}(a)$  improved clover action with a tree level Clover coefficient. Our analysis is based on 73 gauge field configurations generated at  $\beta = 4.1$ , which corresponds to a lattice spacing  $a^{-1} \simeq 1.1$  GeV. The fermion matrix has been inverted at eight different values of the hopping parameter  $\kappa$ . These cover a range of quark masses between  $\sim 30$  MeV and  $\sim 250$  MeV. On each configuration we use four random source vectors at different lattice sites. We thus have a dataset consisting of 292 quark propagators for each quark mass value. Correlation functions were obtained for pi- and rho-meson, as well as for diquark states in the color anti-triplet representation with an attractive q-q interaction and the repulsive color sextet channel<sup>4</sup>.

## 3 Meson Spectral Functions

The spectral functions in pseudo-scalar and vector meson quantum number channels obtained from our analysis using MEM are shown in Fig. 1. In addition to the dominant ground state peaks (pi- and rho-mesons) in the low-energy region, the meson spectral functions show signs of excited states and a broad continuum-like structure at high energies up to the momentum cut-off on the lattice  $\omega_{\max} = \pi/a \sim 3.5$  GeV. We generally find that better statistics and larger  $N_\tau$  result in higher and narrower peaks in the spectral functions which indicates that these correspond to  $\delta$ -function like singularities, *i.e.* poles in the propagator. We also note that in general the ground state contribution is more dominant for lighter quark masses. This is clearly seen in the pseudo-scalar spectral function. On the other hand, the broadening and drop of the low mass contributions seen for the lightest quark masses in the vector spectral function can be addressed to insufficient statistics for this correlator. This is also apparent from conventional exponential fits, which in these cases lead to large errors on the lightest vector meson masses.

Comparing the MEM results with standard two-exponential fits of the correlation functions we find very good agreement. The point of the vanishing pion mass is  $\kappa_c = 0.14922(1)$ , which perfectly coincides with the value 0.14923(2) obtained from a conventional exponential fit. Extrapolating the mass of the rho meson to the chiral limit we obtain  $m_\rho = 0.56(3)$  in lattice units, which should be compared with  $m_\rho(\text{exp-fit}) = 0.58(2)$ .

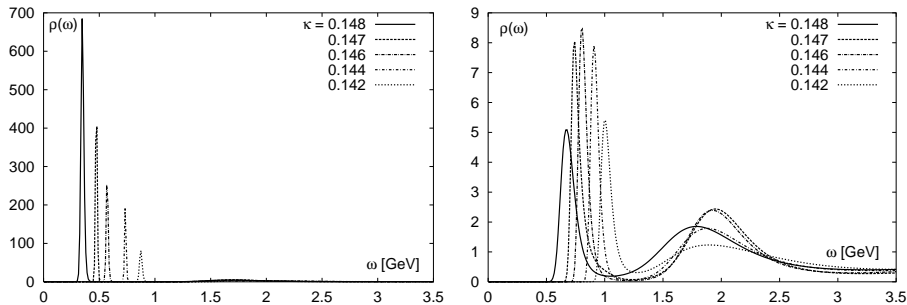


Figure 1: Zero temperature spectral functions for pion (left) and rho meson (right) for different values of the bare quark mass, (note the different  $\rho(\omega)$  scale).

It was shown by the UKQCD group<sup>5</sup> that smeared operators and gauge fields provide a better overlap with the ground state. We applied the fuzzing technique for spatially extended operators with a radius  $R = 0.7$  fm. The spectral functions of the fuzzed mesons show only the ground state peak. They thus uncover unambiguously that the application of the fuzzing technique eliminates the excited states almost completely.

#### 4 Diquark Spectral Functions

We previously had studied diquark correlation functions in Landau gauge<sup>4</sup>. In particular the correlators for color sextet states seemed to be strongly influenced by higher excited states and it was unclear whether a bound state exists at all in these quantum number channels. These difficulties are also show up in our spectral analysis.

Spectral functions similar to those for mesons were obtained for the color anti-triplet diquark states (Fig. 2(a)). In particular the  $(\bar{3}0\bar{3})$  diquark shows a pronounced ground state peak. However, already in the case of the  $(61\bar{3})$  state this ground state peak broadens and becomes comparable in magnitude to the broad continuum structure found at higher energies. This broad continuum becomes even more dominant in the color sextet channels  $(\bar{3}16)$  and  $(606)$  shown in Fig. 2(b). In fact, in the case of color sextet states we find that the spectral function is strongly dependent on the large momentum cut-off  $\omega_{\max}$  used in our analysis. An analysis at smaller lattice spacings thus is needed to better understand the spectral functions in these quantum number channels.

The MEM results for the color anti-triplet diquarks are in good agreement with the masses extracted from two-exponential fits (see Tab. 1). For the color sextet diquarks we observe a deviation in comparison with the 2-mass fits. The

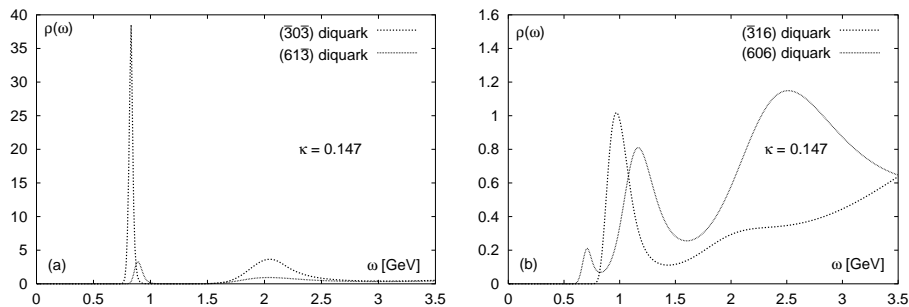


Figure 2: Spectral functions for color anti-triplet (a) and sextet diquark states (b).

mass of the  $\bar{3}16$  diquark has about the same value in the chiral limit, whereas the  $606$  diquark mass obviously is not well represented by a unique mass. This favours the interpretation of color sextet states being unbound, in accordance with the expected repulsive q-q interaction in this channel<sup>4</sup>.

Diquark state	$(\bar{3}0\bar{3})$	$(61\bar{3})$	$(\bar{3}16)$	$(606)$
$ma_{(FSC)}$ : MEM result	0.60(2)	0.70(3)	0.74(9)	—
$ma_{(FSC)}$ : 2-exp. fit	0.62(2)	0.73(4)	0.77(17)	0.50(15)

Table 1: Diquark masses in the chiral limit obtained with MEM and two-exponential fits. Our notation for quantum numbers of the diquark states is (Flavor, Spin, Color)-representation.

## 5 Thermal Spectral Functions

At non-zero temperature meson correlation functions are periodic and restricted to the Euclidean time interval  $[0, 1/T]$ ,

$$D(\tau) = \int_0^\infty d\omega A(\omega) \frac{\cosh(\omega(\tau - 1/2T))}{\sinh(\omega/2T)} .$$

In the high temperature limit the meson spectral functions are expected to approach those of freely propagating quark anti-quark pairs. To leading order this is described by the free spectral function, *i.e.*  $A(\omega) = \frac{N_c}{4\pi^2} \omega^2 \tanh(\omega/4T)$  in the scalar channel. We want to test here whether this behaviour can be reproduced on lattices with finite temporal extent  $N_\tau$ . We use the continuum expression for  $D(\tau)$  and evaluate it at a discrete set of Euclidean times,  $\tau_k = k/N_\tau$ , with  $k = 1, 2, \dots, N_\tau - 1$ . This is shown in Fig. 3(a). The reconstructed spectral functions in Fig. 3(b) were obtained with MEM, adding Gaussian noise with the variance  $\sigma(\tau) = b D(\tau)/\tau$  to the exact results.

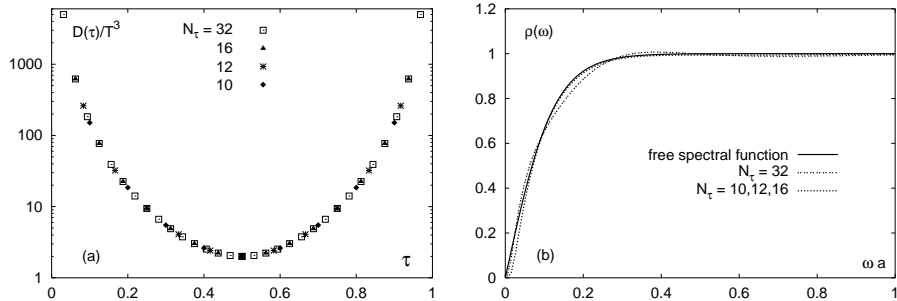


Figure 3: Free thermal meson correlation function at Euclidean times  $\tau \equiv \tau_k = k/N_\tau$  for different  $N_\tau$  (a) and the reconstructed spectral function (b). For the reconstruction shown in (b) different subsets of the data shown in (a) have been used as indicated. The noise level on the data has been set to  $b = 0.01$ .

We note that one can reproduce the shape of the spectral function quite well already from correlation functions calculated at  $N_\tau = 16$  points. However, twice as many data points are needed for a good quantitative description of  $\rho(\omega)$ . One thus may expect that the reconstruction of the continuum part of thermal correlation functions based on simulations on lattices with temporal extent  $N_\tau$  will require information on the correlation functions at  $\mathcal{O}(30)$  points. This may either be achieved by performing calculations on large temporal lattices or by combining information from lattices with different temporal extent but fixed temperature.

## 6 Conclusions

We find that the application of MEM to the analysis of lattice correlation functions does yield useful additional information to that of conventional exponential fits. It can lead to quantitative results on pole and continuum contributions to spectral functions.

## References

1. for a review see: M. Jarrel and J.E. Gubernatis, *Physics Reports* **269**, 133 (1996).
2. Y. Nakahara *et al.*, *Phys. Rev. D* **60**, 091503 (1999) and *Nucl. Phys. B* (Proc. Suppl.) **83-84**, 191 (2000).
3. R. K. Bryan, *European Biophysics Journal* **18**, 165 (1990).
4. M. Heß *et al.*, *Phys. Rev. D* **58**, 111502 (1998).
5. P. Lacock *et al* (UKQCD), *Phys. Rev. D* **51**, 6403 (1995).